arXiv:1703.07620v1 [math.AG] 22 Mar 2017

THE TROPICAL SUPERPOTENTIAL FOR $\mathbb{P}^2$

THOMAS PRINCE

Abstract. We present an extended worked example of the computation of the tropical superpotential considered by Carl–Pumperla–Siebert [8]. In particular we consider an affine manifold associated to the complement of a non-singular genus one plane curve, and calculate the wall and chamber decomposition determined by the Gross–Siebert algorithm. Using results of [8] we determine the tropical superpotential, via broken line counts, in every chamber of this decomposition. The superpotential defines a Laurent polynomial in every chamber, which we demonstrate to be identical to the Laurent polynomials predicted by [10] to be mirror to $\mathbb{P}^2$.

1. Introduction

The phenomenon of Mirror Symmetry famously identifies pairs of dual Calabi–Yau manifolds, as predicted by a duality of $N = 2$ superconformal sigma models with Calabi–Yau target spaces. The phenomenon of Mirror Symmetry extends to some non-Calabi–Yau cases, in particular to the case of *Fano manifolds* [11–13, 22]. In this setting Mirror Symmetry is expected to relate a pair (X, D) of a Fano manifold X and $D \in |-K_X|$ with a *Landau–Ginzburg model* $(X^\vee, W)$, consisting of a complex manifold $X^\vee$ and holomorphic function W.

The prototypical example of Mirror Symmetry for Fano manifolds is the case $(\mathbb{P}^2, D)$ where D is the toric boundary of $\mathbb{P}^2$. The mirror Landau–Ginzburg model in this case is the pair

$$\big(\mathbb{C}^{\star 2}, x + y + \tfrac{1}{xy}\big).$$

Many mathematical formulations of Mirror Symmetry can be proved in this setting including Homological Mirror Symmetry [7, 32, 33], the Strominger–Yau–Zaslow (SYZ) conjecture [9], as well as the original formulation of Givental [13]. However, even in the case of $(\mathbb{P}^2, E)$ where E is a non-singular genus one curve, the subject of this article, the SYZ formulation of Mirror Symmetry, is highly non-trivial.

In general, given a Fano manifold X the SYZ Conjecture [34] predicts – see for example the surveys [5,6] – that the variety $X^\vee$ is a moduli space of pairs (L, ∇), where L is a special Lagrangian torus in X and ∇ a $U(1)$ connection on L. Moreover, it is expected that W is a count of Maslov index two holomorphic discs in X whose boundary in contained in L. One important aspect of Mirror Symmetry from the perspective of the SYZ conjecture is that the moduli space of special Lagrangians on X carries a pair of dual *affine structures*. (See Definition 4.1.)

Fundamental work of Kontsevich–Soibelman [25] and Gross–Siebert [20] exploits this connection between Mirror Symmetry and affine geometry: the authors directly construct a degeneration of a mirror variety via an essentially combinatorial construction (scattering) on an affine manifold. Returning to the case of $\mathbb{P}^2$ one can consider an affine manifold $B_{\mathbb{P}^2}$ formed by 'smoothing the corners' of the moment polytope as shown in Figure 1.1. This operation appears in [8, 31] and is explored in some detail in [30]. There is also an analogue of the superpotential W, the *tropical superpotential* introduced in [8], in which holomorphic disc counting is replaced by counting of tropical discs or *broken lines* in the Legendre dual affine manifold $B^\vee_{\mathbb{P}^2}$ (see Section 5). This builds on the general

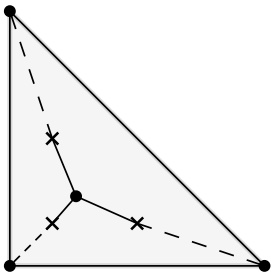

FIGURE 1.1. Intersection complex for a toric degeneration of $(\mathbb{P}^2, E)$

correspondence between tropical and holomorphic curves established by Mikhalkin [26,27] and Nishinou–Siebert [29].

One essential feature of the Gross–Siebert algorithm is that it encodes the data used to define a degeneration in terms of walls of a certain wall and chamber decomposition of an affine manifold, created in an order-by-order scattering process. In this article we determine the wall and chamber structure on $B^\vee_{\mathbb{P}^2}$ produced by the Gross–Siebert algorithm and, using results of [8], determine the tropical superpotential in every chamber.

Theorem 1.1. *Given the affine manifold $B^\vee_{\mathbb{P}^2}$ we can construct a* compatible structure[1] *$\mathscr{S}$ via the Gross–Siebert algorithm. The structure $\mathscr{S}$ determines, for each k, a polyhedral decomposition $\mathscr{P}_k$ of $B^\vee_{\mathbb{P}^2}$, and we write* $\mathrm{Chambers}(\mathscr{S}, k)$ *for the set of maximal cells of $\mathscr{P}_k$. There is a domain $U = \bigcup_{k\geq 0} U_k \subset B^\vee_{\mathbb{P}^2}$ such that:*

- *For all $j \geq k$, the restriction of $\mathscr{P}_j$ to $\bar{U}_k$ is a constant union of chambers $\mathfrak{u} \in \mathrm{Chambers}(\mathscr{S}, k)$.*
- *Each $\mathfrak{u} \in \mathrm{Chambers}(\mathscr{S}, k)$ such that $\mathfrak{u} \subset \bar{U}_k$ is a triangle similar to a Fano polygon $P_\mathfrak{u}$ defined by the spanning fan of the central fiber of a toric degeneration of $\mathbb{P}^2$.*
- *The union of the support of rays of $\mathscr{S}^k$ for all $k \geq 0$ restricted to $B^\vee_{\mathbb{P}^2}\backslash U$ is dense.*

We refer to [15,20] for the precise definitions of these terms though we recall them briefly in Section 4. Combining Theorem 1.1 with the results of [8] we recover the tropical superpotential in every chamber.

Theorem 1.2. *The* tropical superpotential *(defined in Section 4) $W^k_{\omega,\tau,\mathfrak{u}}$ is* manifestly algebraic*, in the sense of [8], and may be identified with the rigid maximally mutable Laurent polynomial (as defined in [1]) with Newton polygon $P_\mathfrak{u}$.*

In particular we observe that $B^\vee_{\mathbb{P}^2}$ contains a region densely covered with rays and the complement of this region has a wall and chamber structure. Thus, rather than a single Laurent Polynomial W, as in the case of the pair $(\mathbb{P}^2, D)$, there are infinitely many polynomials W related by certain birational changes of variables. The dual cell complex to these walls and chambers is a trivalent tree, and each chamber is a triangle similar to the Fano triangle defined by the corresponding degeneration of the projective plane. In fact the nodes of this trivalent tree have an interpretation as integral solutions of the Markov equation $x^2 + y^2 + z^2 = 3xyz$. Indeed, we recall that toric degenerations of $\mathbb{P}^2$ are also classified by such Markov triples; see [21].

[1] See Section 4.

Theorem 1.3. *The set of toric varieties to which* $\mathbb{P}^2$ *admits a toric degeneration is in canonical bijection with the integral solutions of the* Markov equation $a^2+b^2+c^2=3abc$. *Consequently all toric degenerations of* $\mathbb{P}^2$ *are related by combinatorial mutation.*

We recall that combinatorial mutation was defined in [4] for any Fano polytope[2]. The Markov equation is well known and appears in many different areas of mathematics. The integral solutions of this equation are completely described by the following lemma.

Lemma 1.4. *Given a solution* (a,b,c) *of* $x^2+y^2+z^2=3xyz$ *another solution is given by* $\left(b,c,\frac{3bc-a^2}{a}\right)$. *Given the initial solution* $(1,1,1)$ *this process generates all integral solutions to the Markov equation.*

Thus the solutions of the Markov equation may be encoded in a trivalent graph $\mathcal{G}$, in which each node is a triple (a,b,c) solving the Markov equation. Starting from the initial solution $(1,1,1)$ one may inductively define a *distance* $\mathrm{dist}(v), v \in \mathrm{verts}(\mathcal{G})$, of a node from $(1,1,1)$ via successive mutations.

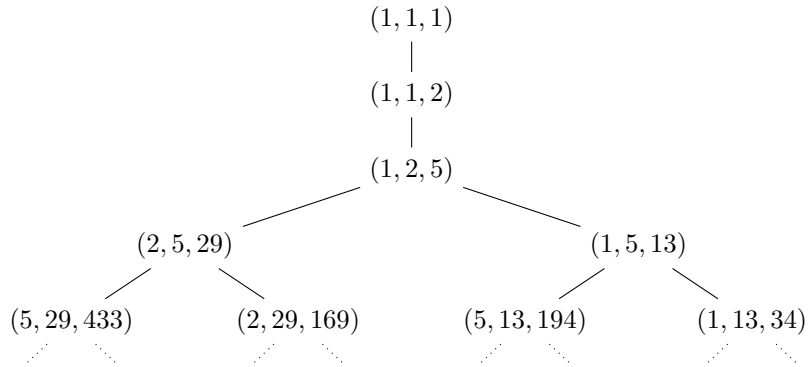

In fact this structure on the mirror to the projective plane is expected from another point of view on Mirror Symmetry. Following [10], one expects that periods of the fibration defined by W computes a certain generating function of Gromov–Witten invariants called the (regularised) *quantum period*. In the case of $\mathbb{P}^2$ it is easy to construct an infinite family of Laurent polynomials $f \in \mathbb{C}[\mathbb{Z}^2]$ such that the period integral

$$\pi_f(t) := \int_\Gamma \frac{\Omega}{1-tf},$$

where $\Gamma := \{|x_1| = |x_2| = 1\}$ and $\Omega := \frac{1}{2\pi\imath}\frac{dx_1}{x_1} \wedge \frac{dx_2}{x_2}$, is equal to the regularised quantum period $\widehat{G}_{\mathbb{P}^2}$ of $\mathbb{P}^2$,

$$\widehat{G}_{\mathbb{P}^2}(t) = \sum_{m\geq 0} \frac{(3m)!}{(m!)^3} t^{3m}.$$

Indeed, following [10] we say that a Laurent polynomial $f \in \mathbb{C}[\mathbb{Z}^2]$ is *mirror-dual* to $\mathbb{P}^2$ if its period $\pi_f(t)$ is equal to the regularised quantum period of $\mathbb{P}^2$. Such polynomials are classified [2] and are in bijection with toric degenerations of $\mathbb{P}^2$. Theorem 1.2 shows that all Laurent polynomials mirror-dual to $\mathbb{P}^2$ can be expressed as counts of broken lines in the affine manifold $B^\vee_{\mathbb{P}^2}$.

Finally we observe that the integral solution to the Markov equation also enumerate the monotone Lagrangian tori in $\mathbb{P}^2$ found by Vianna [35]. In fact Theorems 1.1 and 1.2 can be interpreted as tropical analogues of these results in symplectic geometry. Indeed, for each chamber in $B^\vee_{\mathbb{P}^2}$ the SYZ conjecture predicts there is a family of Hamiltonian isotopic Lagrangian tori lying in $\mathbb{P}^2$, thus we demonstrate the close compatibility in this case of the

[2]That is, a polytope with primitive integral vertices containing the origin in its interior.

wall and chamber structure defined by the Gross–Siebert algorithm and that predicted by the existence of non-Hamiltonian isotopic Lagrangian tori.

2. A Normal Form for Fano Polygons

In this section we study the class of polygons associated[3] to the $\mathbb{Q}$-Gorenstein toric degenerations of $\mathbb{P}^2$. In fact all these polygons are related by combinatorial mutation and we refer to this collection of polygons as the *mutation class of* $\mathbb{P}^2$. We refer to [4] for the general definition of a combinatorial mutation, but in our particular setting the definition simplifies considerably and in Lemma 2.3 we give an elementary characterisation of the definition. To any Fano polygon one can assign a *singularity content* [3] $(n, \mathcal{B})$ consisting of an integer n and set of cyclic quotient singularities $\mathcal{B}$. The combinatorial definition and proof of mutation invariance is given in [3], but in [1] it was observed that the invariant has a geometric interpretation. In particular, given a Fano polygon P and X a locally $\mathbb{Q}$-Gorenstein rigid del Pezzo surface which admits a $\mathbb{Q}$-Gorenstein degeneration to X_P, the integer n is the topological Euler characteristic of the smooth locus of X and $\mathcal{B}$ is the basket of singularities of X.

The class of Fano polygons of $\mathbb{Q}$-Gorenstein toric degenerations of $\mathbb{P}^2$ is well-understood. Indeed, combining the results of [21] and [2] we have the following theorem.

Theorem 2.1. *Given a Fano polygon P the following are equivalent:*

(1) P is the polygon of a degeneration of $\mathbb{P}^2$.
(2) The singularity content of P is $(3, \varnothing)$.
(3) The polygons P and $P_0 := \operatorname{conv}((1,0),(0,1),(-1,-1))$ are related by a sequence of combinatorial mutations.

Remark 2.2. Theorem 2.1 implies that the polygon P of a toric surface X_P which admits a $\mathbb{Q}$-Gorenstein smoothing to $\mathbb{P}^2$ is a triangle. Performing any mutation out of P completely removes an edge and a new edge appears at the opposite vertex.

Lemma 2.3. *Given a Fano polygon $P \subset N_{\mathbb{Q}}$ with singularity content $(3, \varnothing)$ a mutation of P with weight vector $w \in M$, and factor $F = \operatorname{conv}((0,0), f) \subset w^{\perp}$ is the Fano polygon* $\operatorname{mut}(P, F)$ *defined in two steps:*

(1) fix an edge E of P with vertices v_+, v_- such that $\langle v_+ - v_-, w\rangle > 0$,
(2) define $\operatorname{mut}_w(P, F)$ *to be* $\operatorname{conv}(v_+, v_-, v)$ *where $v := v_+ + \langle w, v_+\rangle f$.*

Remark 2.4. Combinatorial mutation is the operation on polytopes induced by taking the Newton polytopes of Laurent polynomials related by certain birational transformations called *algebraic mutations*[4] [4]. In the two-dimensional case these are precisely those birational transformations $\theta_{w,F}$

$$\theta^{\star}_{w,F}(z^n) = F^{\langle w,n\rangle} z^n,$$

where $F = (1 + z^f)$ and $f \in w^{\perp}$ is a primitive lattice point.

The effect of a mutation on the triple of dual vectors defining the edges of P is similarly straightforward. As shown in Figure 2.1, the inward-pointing normal w_3 to the mutating edge changes sign, and the remaining pair undergo a piecewise linear map in which one is fixed and the other undergoes a shear with invariant direction spanned by w_3.

Lemma 2.5. *Given a Fano polygon P with singularity content $(3, \varnothing)$ a mutation of P is exactly (i.e. not only up to* $\mathrm{GL}(2,\mathbb{Z})$*) determined by a* mutating *edge E and* fixed *edge E'.*

[3]We say a polygon P is associated to a toric variety X if X is isomorphic to the toric variety defined by the fan formed by taking cones over the faces of P.
[4]These are also called *symplectomorphisms of cluster type* [24].

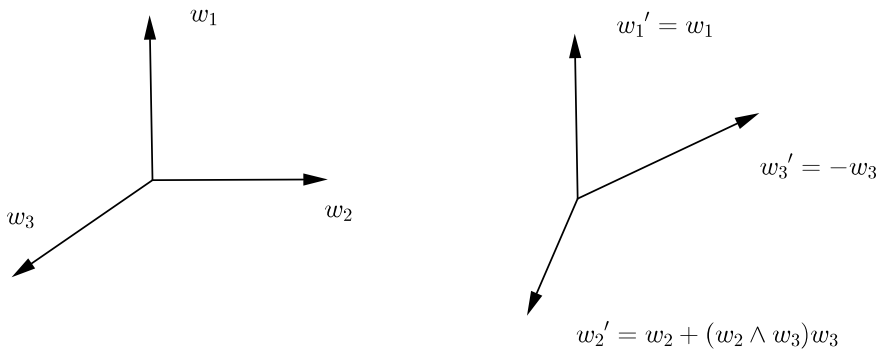

FIGURE 2.1. Normal vectors changing under a mutation

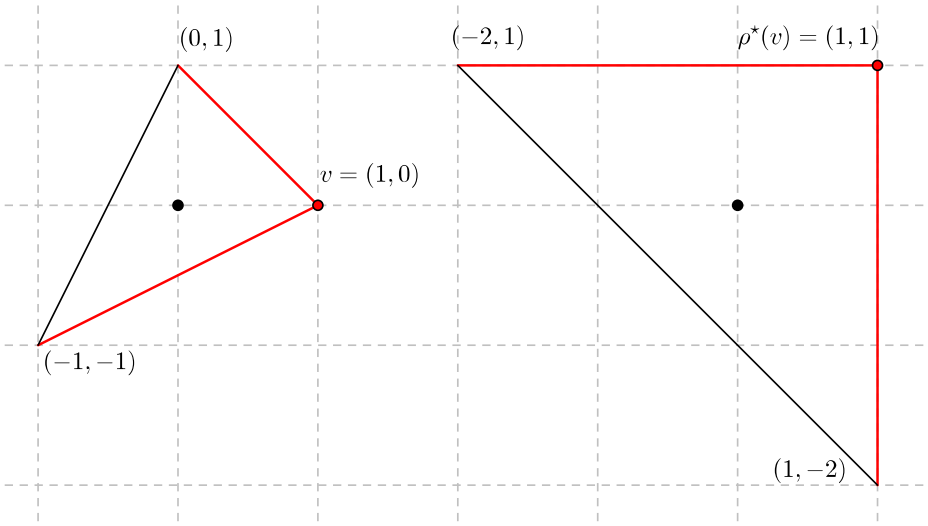

FIGURE 2.2. A triangle in normal form

Given a triangle P with singularity content $(3, \varnothing)$ and a vertex $v \in \text{verts}\,(P)$, we describe a 'normal form' for P making these edges orthogonal, at the expense of embedding P into a finer lattice.

Definition 2.6. Given a pair (P, v), $v \in \text{verts}\,(P)$ let E_1, E_2 be the edges incident to v and let w_1, $w_2 \in M$ be their normal vectors respectively. Consider the map

$$\rho\colon \mathbb{Z}^2 \to M \qquad\qquad \rho\colon e_i \mapsto w_i, \text{ for } i = 1, 2$$

where e_i are elements of the standard basis. The dual map $\rho^\star\colon N \hookrightarrow \mathbb{Z}^2$ embeds N into the lattice $\mathbb{Z}^{2\vee}$, consequently P is embedded in the new lattice $\mathbb{Z}^{2\vee}$ with fixed coordinate directions. We refer to the embedding $\rho^\star$ as the *normal form* for (P, v).

Figure 2.2 shows the Fano polygon associated to $\mathbb{P}^2$ in standard form.

Remark 2.7. This construction is intimately related to the construction of a *cluster algebra* associated to P, [23] c.f. [16]. There one defines *seed data* by fixing the lattice $\mathbb{Z}^m$ with its standard basis, and define a skew-symmetric bilinear form on $\mathbb{Z}^m$. The mutation of seed data then involves making a choice of basis vector, for example e_k, and transforming this basis to:

$$e_i' = \begin{cases} -e_k & \text{if } i = k \\ e_i + \max(e_k \wedge e_i, 0).e_k & \text{otherwise} \end{cases}$$

Given any Fano polygon P with singularity content $m_P = \sum_E m_E$, where m_E is the singularity content[5] of cone(E) and the sum is over the edges of P, we can define a map $\hat{\rho}\colon \mathbb{Z}^{m_P} \to M$ sending m_E basis vectors to the inward-pointing normal vector to the edge E. We can then form a skew-symmetric matrix $(u_1, u_2) := \hat{\rho}(u_1) \wedge \hat{\rho}(u_2)$. Restricting this definition to a pair of basis vectors we recover our previous definition of ρ.

Notation 2.8. We fix notation for the local index of various cones that appear in P and its mutations in E_1, E_2 respectively.

- Let ℓ_i be the local index of the cone over the edge E_i.
- Let ℓ_i'be the local index of the cone over the edge E_i'. Where E_i' is the new edge formed by mutating the edge E_i.
- Let $L_i = \ell_i + \ell_i'$.

Putting P in normal form embeds the edges E_i of P into affine coordinate lines. This means we have a very simple description of the result of the pair of mutations in E_i for $i = 1, 2$. To make this precise we need to define what it means for a polygon to mutate *with respect to a sublattice.*

Definition 2.9. Given a sublattice $\rho^\star\colon N \hookrightarrow \mathbb{Z}^2$ and P a polygon in N, a vector $w \in \mathbb{Z}^{2\star}$ and a polygon $F = \rho^\star(F')$ for a polygon $F' \subset w^\perp$ of $\rho^\star(P)$ we define the *mutation with respect to* N

$$\mathrm{mut}_{w,\rho^\star}(\rho^\star(P), F) := \rho^\star(\mathrm{mut}_{\rho(w)}(P, F))$$

We prove two lemmas which will simplify our future calculations considerably.

Lemma 2.10. *Given a Fano polygon P with singularity content $(3, \varnothing)$ put P in normal form with respect to $v \in \mathrm{verts}(P)$, incident to the edges E_1, E_2. The two corresponding mutations of $\rho^\star(P)$ with respect to N have factors*

$$F_1 = \mathrm{conv}((0,0),(s,0)) \qquad F_2 = \mathrm{conv}((0,0),(0,s))$$

respectively, where s is the index $[\mathbb{Z}^2 : N]$.

Proof. The factors F_i are, by definition, line segments, with one vertex at the origin. Since F_i lies in $w_i^\perp$,

$$F_1 = \mathrm{conv}((0,0),(k_1,0)) \qquad F_2 = \mathrm{conv}((0,0),(0,k_2))$$

for some k_i. To see that $k_i = s$ for $i = 1, 2$ we observe that

$$k_1 = \langle (1,0), \rho^\star(v_1)\rangle = \rho^\star(v_1)(1,0) = v_1(\rho(1,0)) = \langle w_2, v_1\rangle$$

where $v_i \in \mathrm{verts}(P)$ is incident to E_i and not equal to v. Using the non-degenerate pairing the functional $\langle -, v_1\rangle\colon M \to \mathbb{Z}$ is equal to the functional $w_1 \wedge -$. But $w_1 \wedge w_2 = s$ by the definition of the map ρ. □

Lemma 2.11. *Given a Fano polygon P with singularity content $(3, \varnothing)$ fix a pair of edges E_1, E_2, then $L_1/\ell_2 = L_2/\ell_1 = s$.*

[5]See [3] for the definition of the singularity content of a cone; it is very closely related to the Milnor number.

Proof. Since the cones over the distinguished edges E_1 and E_2 are primitive T-cones, the mutation in these edges completely removes the edge. Consequently the mutation of $\rho^\star(P)$ with respect to N also removes an entire edge. Thus, while the local index of the cones over $\rho^\star(E_i)$ remains unchanged, the width $L_1 = w = rs$, where the second equality follows from Lemma 2.10. However, for example, for the cone over E_1, $w = L_1$ and $r = \ell_2$. The analogous consideration for E_2 completes the proof. □

3. Scattering Diagrams from Combinatorial Mutations

We now turn to a construction of the support of a scattering diagram[6] in terms of combinatorial mutations. We shall build a collection of triangles using successive mutations and use the edges of these polygons to define a sequence of rays. In the next section we shall directly compare this with the rays of a certain simple scattering diagram. The collection of triangles we consider in this section fit together into an embedded simplicial complex which we refer to as a *diagram*.

Definition 3.1. Given a triple (P, v, k) where P is a Fano polygon P with singularity content $(3, \varnothing)$, $v \in \operatorname{verts}(P)$ and $k \in \mathbb{Z}_{\geq 0}$. Let E_1, E_2 denote the edges of P adjacent to v and let E denote the opposite edge to v, and allow this labelling to persist after mutation. We define a *diagram* $\operatorname{Diag}_k(P, v) := (\mathscr{P}_k(P, v), \iota_{P,v,k})$, where

- $\mathscr{P}_k(P, v)$ is a two-dimensional simplicial complex with $2k + 1$ maximal cells and;
- $\iota_{P,v,k} \colon |\mathscr{P}_k(P, v)| \to \mathbb{R}^2$ is a continuous map from a geometric realisation of $\mathscr{P}_k(P, v)$ to $\mathbb{R}^2$.

Denote the chambers of $\mathscr{P}_k(P, v)$ by $\mathfrak{u}_{k,0}$, $\mathfrak{u}^i_{k,j}$ for $i \in \{1, 2\}$ and $1 \leq j \leq k$ (suppressing the dependence on P and v). We fix $\mathscr{P}_k(P, v)$ by requiring that:

- The following intersections each consist of exactly one edge of the respective chambers,
  - $\tau_{i,j} := \mathfrak{u}^i_{k,j} \cap \mathfrak{u}^i_{k,j-1}$ for $1 \leq j \leq k$
  - $\tau_{i,0} := \mathfrak{u}^i_{k,1} \cap \mathfrak{u}_{k,0}$
- Every chamber $\mathfrak{u}^i_{k,j}$ contains the distinguished vertex v.

We fix the map $\iota_{P,v,k}$ by requiring that,

- $\iota_{P,v,k} \colon \mathfrak{u}_{k,0} \to P$ isomorphically.
- Up to scale and translation $\iota_{P,v,k}(\mathfrak{u}^i_{k,1})$ is equal to the mutation of P with mutating edge E_i and fixed edge E_{3-i}.
- For $1 \leq j \leq k$, up to scale and translation $\iota_{P,v,k}(\mathfrak{u}^i_{k,j})$ is equal to the mutation of the Fano polygon corresponding to $\mathfrak{u}^i_{k,j-1}$ with mutating edge $E_{a_{i,j}}$ and fixed edge E. Here $a_{i,j}$ is defined by the requirement that $a_{i,j+1} = 3 - a_{i,j}$ and $a_{i,0} = i$.

In Figure 3.1 we give a schematic example of $\operatorname{Diag}_3(P, v)$ (for P in normal form with respect to v). The remainder of this section is devoted to showing that for any P, v and k, $\iota_{P,v,k}$ is an embedding.

To describe the slopes of the rays in $T_v\mathbb{R}^2$ induced by $\operatorname{Diag}_k(P, v)$ we use the description of the mutation of the normal vectors to describe the normal vectors of the region $\mathfrak{u}^i_{k,j}$.

Definition 3.2. Define $u^{i,1}_j$, $u^{i,2}_j \in M$ to be the normal vectors to the edges E_1, E_2 of $\mathfrak{u}^i_{k,j}$ (for any $k > j$) respectively.

[6] See Section 4 for a special case and [15, 19, 20] for more details.

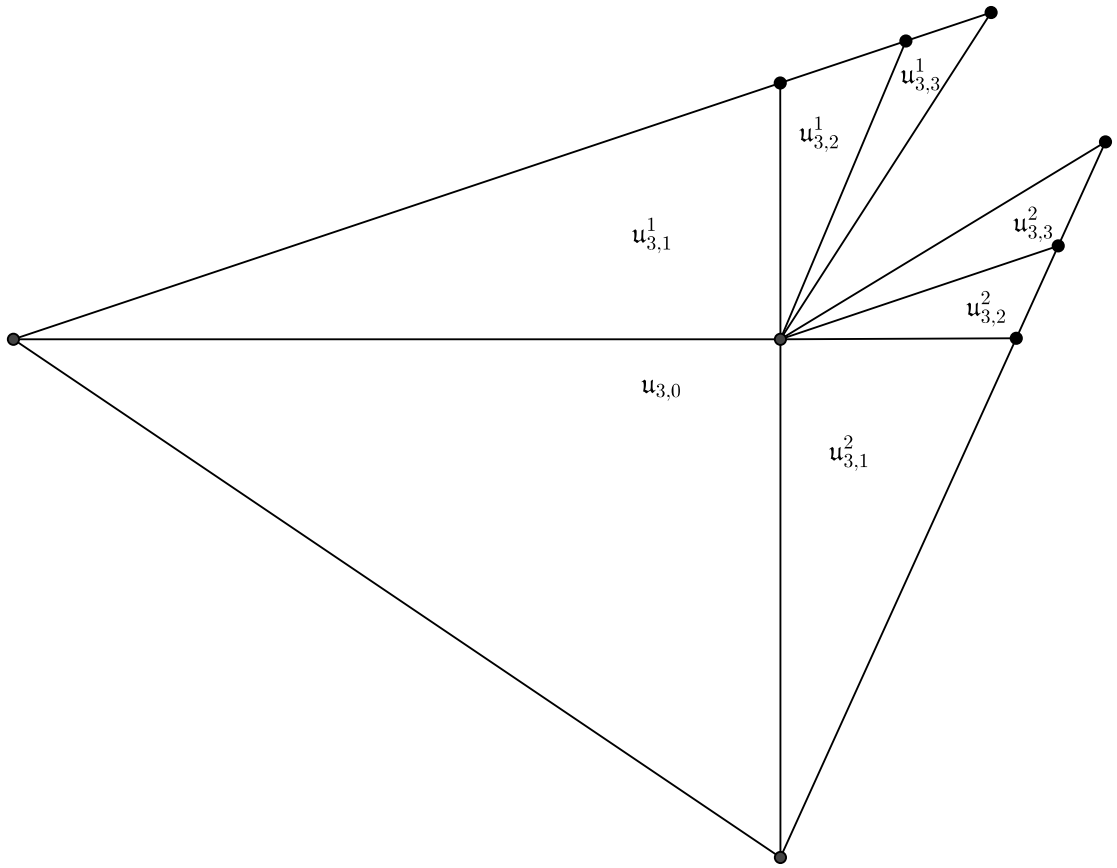

FIGURE 3.1. A schematic picture of $\mathrm{Diag}_3(P, v)$

The first few terms of $u_j^{1,1}$, $u_j^{1,2} \in \mathbb{Z}^2$ are:

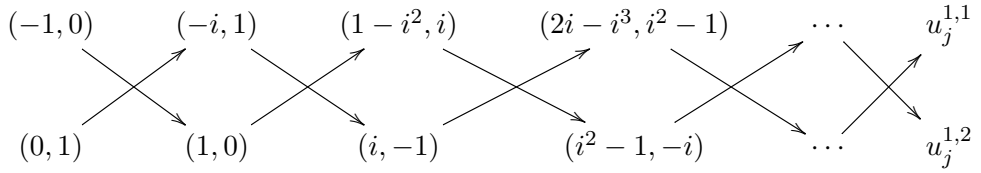

There is an analogous sequence for the terms $u_j^{2,l}$. From the piecewise linear map in M it is easy to determine that

$$u_k^{1,1} = (-a_{k+1}, a_k), u_k^{1,2} = (a_k, -a_{k-1})$$

where the a_k satisfy the recursive relationship:

$$a_{k+1} = sa_k - a_{k-1}$$

Lemma 3.3. *These normal vectors define lines in $\mathbb{R}^2$ which converge to a line with slope $\frac{-s+\sqrt{s^2-4}}{2}$*

Proof. Straightforward calculation. □

Remark 3.4. Making this calculation for the sequence $u_k^{2,l}$, the sequence of slopes of the induced lines converges to $\frac{-s-\sqrt{s^2-4}}{2}$.

Next we compute the slopes of the rays in $T_v\mathbb{R}^2$ generated by edges of the chambers $\mathfrak{u}_{k,j}^i$.

Definition 3.5. Let v_j^i be the set of vectors generating a sequence of ray $\mathfrak{d}_j^i$ defined recursively as follows.

- $v_1^1 := (-1, 0)$, $v_2^1 := (0, 1)$
- $v_1^2 := (0, -1)$, $v_2^2 := (1, 0)$
- $v_{j-1}^i + v_{j+1}^i = sv_j^i$, recalling that $s = \det(\rho)$.

We record the following easy comparison result,

Lemma 3.6. *The set of rays generated by $v_j^{i,l}$ in $T_v\mathbb{R}^2$ is equal to that induced on $T_v\mathbb{R}^2$ by the chambers $\mathfrak{u}_{k,j}^i$ for $i = 1, 2$, for all $j \geq 1$, $k \geq j$.*

Proof. This follows immediately from our considerations of the normal vectors after taking the orthogonal directions using the volume form $(- \wedge -)$. □

In particular these rays converge to a pair of asymptotes:

Lemma 3.7. *The sequence of rays $\mathfrak{d}_j^i$ converge to the ray $\mathfrak{d}_\infty^i$ with slope*

$$g_\infty^i := \frac{s \pm \sqrt{s^2 - 4}}{2}$$

where $i = 1$ corresponds to the asymptote with positive sign.

Proof. These are the orthogonal directions to the rays in $M_\mathbb{R}$ obtained in Lemma 3.3. □

Next consider the union of the fixed edges E of $\mathfrak{u}_{j,k}^i$. This defines a pair of rays in $\mathbb{R}^2$ which we denote by $\mathfrak{e}_i$. In order to prove $\iota_{P,v,k}$ is an embedding we require a bound on the gradient of $\mathfrak{e}_i$. This bound makes use of the fact that P has singularity content $(3, \varnothing)$ and thus is of the form $\mathbb{P}(a^2, b^2, c^2)$. Our first step is to relate the triple of weights (a, b, c) for defined by P to the numbers ℓ_1, ℓ_2, s.

Lemma 3.8. *Given a triangle mutation equivalent to $\mathbb{P}^2$ in standard form with respect to the vertex corresponding to a, let the other two vertices in clockwise order correspond to b and c then $\ell_1 = b$, $\ell_2 = c$ and $s = 3a$.*

Proof. That $s = 3a$ is clear from the definition since fixing the two edges adjacent to the distinguished vertex as E_1, E_2, $s = \det(\rho) = \rho(E_1) \wedge \rho(E_2)$. To prove $\ell_1 = b$ and $\ell_2 = c$ recall that ℓ_i is the height (or local index) of the edges E_1, E_2 respectively and observe that for a Fano polygon P such that $X_P = \mathbb{P}(a^2, b^2, c^2)$ such that $a^2 + b^2 + c^2 = 3abc$, the triple of local indices is given by (a, b, c). □

The main technical result of this section tells us that once the rays $\mathfrak{e}_i$ enter the region defined by the pair of asymptotes of the two sequences of rays v_∞^i they never emerge again.

Proposition 3.9. *For $i = 1, 2$ denote the slope of the ray $\mathfrak{e}_i$ by g_i, then:*

$$g_\infty^1 \geq g_i \geq g_\infty^2$$

Proof. First we need to compute the gradient of the rays $\mathfrak{e}_i$. Considering the initial chamber $\mathfrak{u}_{k,0}$ the edge e opposite v has normal vector (ℓ_1, ℓ_2). Consequently the normal directions to E in the chambers $\mathfrak{u}_{k,1}^i$ are $(\ell_1, \ell_2 - s\ell_1)$ and $(\ell_1 - s\ell_2, \ell_2)$ for $i = 1, 2$ and $k \geq 1$. Thus the orthogonal lines in N have slopes $\frac{\ell_1}{s\ell_1 - \ell_2}$ and $s - \frac{\ell_1}{\ell_2}$. As we can interchange b

and c this situation is symmetric and we need only consider the second case, i.e. we only need to prove that

$$\frac{s-\sqrt{s^2-4}}{2} \leq s - \frac{\ell_1}{\ell_2} \leq \frac{s+\sqrt{s^2-4}}{2}$$

By Lemma 3.8 these are equivalent to the inequality

$$\sqrt{(3a)^2-4} \geq \left|3a - \frac{2b}{c}\right|$$

But squaring both sides and rearranging we may reduce this inequality to a tautology:

$$\begin{aligned}(3a)^2 - 4 > (3a)^2 - 4.3\frac{ab}{c} + 4\frac{b^2}{c^2} \Leftrightarrow \\ \frac{b}{c}\left(\frac{3ac-b}{c}\right) > 1 \Leftrightarrow \\ 1 + \frac{a^2}{c^2} > 1\end{aligned}$$

□

Corollary 3.10. *The map $\iota_{P,v,k}$ is an embedding for every triple (P, v, k).*

In the proof of Theorem 1.1 we will make use of a gluing construction, whereby $\mathrm{Diag}(P, v, k)$ is created from iterated embeddings of $\mathrm{Diag}(P_i, v_i, 1)$ where P_i and v_i form a sequences of embedded polygons and vertices.

Construction 3.11. Given a diagram, $\mathrm{Diag}(P, v, k)$ define $P_k^1 := \mathfrak{u}_{k,k}^1$ and $P_k^2 := \mathfrak{u}_{k,k}^2$. Further, let v_k^1 and v_k^2 denote the vertices of P_k^1 and P_k^2 respectively such that $v_k^i \notin \mathrm{verts}\left(\mathfrak{u}_{a,b}^i\right)$ for any $(a, b) \neq (k, k)$. There are Fano polygons $\tilde{P}_k^i$ associated with P_k^i for $i = 1, 2$ such that the normal directions of $\tilde{P}_k^i$ coincide with those of P_k^i. Forming the diagram $\mathrm{Diag}(\tilde{P}_k^i, v_k^i, 1)$ and composing the embedding $\iota_{P_k^i, v_k^i}$ with a scale and translation, we can ensure that

$$\iota_{\tilde{P}_k^i, v_k^i}(\tilde{P}_k^i) = P_k^i$$

The simplical complex underlying $\mathrm{Diag}(P_k^i, v_k^i, 1)$ has two other chambers which extend the simplicial complex $\mathrm{Diag}(P, v, k)$. In fact, extending $\mathrm{Diag}(P, v, k)$ by the chambers $\mathfrak{u}_{1,1}^{2-i}$ of $\mathrm{Diag}(P_k^i, v_k^i, 1)$ we obtain the embedded complex $\mathrm{Diag}(P, v, k+1)$. An example of the process is shown in Figure 3.11

Eventually we shall want to mutate not just E_1 and E_2 but the third edge as well, to do this we shall need to recursively apply the construction we have just described to various triangular regions. However, before we describe this construction we will give a different interpretation of the set of rays we have defined, in a somewhat ad hoc fashion, in this section. That is, we shall describe this set of rays as a subset of the rays of a *scattering diagram.*

4. Background On the Gross–Siebert Algorithm

In this section we briefly recall the main definitions, results, and notation used in the Gross–Siebert algorithm; we refer to [20] for full details. The Gross–Siebert algorithm takes as input a 'discrete' part and a 'continuous' part. The discrete part comprises a tuple $(B, \mathscr{P}, s, \phi)$ where:

(1) B is an integral affine manifold with singularities,
(2) $\mathscr{P}$ is a polyhedral decomposition,
(3) s is open gluing data, defined in [20] and,
(4) ϕ is a multi-valued piecewise linear function on B, referred to as a *polarization.*

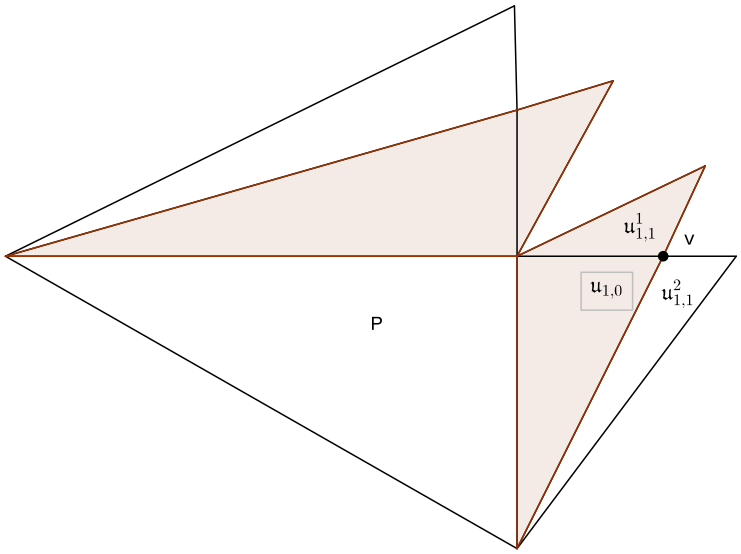

FIGURE 3.2. Gluing copies of $\mathrm{Diag}(P_i, v_i, 1)$ to form $\mathrm{Diag}(P, v, k)$

Definition 4.1. An integral affine manifold with singularities is a topological manifold B, an open dense submanifold $B_0 \subset B$ such that $\Delta := B \backslash B_0$ has codimension at least two, and an atlas on B_0 such that all transition functions lie in the group of affine functions $\mathrm{GL}(2,\mathbb{Z}) \ltimes \mathbb{Z}^2$.

Observe that in B_0 linear objects (lines, polyhedra) are well defined and the notion of a polyhedral decomposition is well-defined. The continuous part consists of a collection of *slab functions* f_τ. Given τ, a codimension one piece of $\mathscr{P}$, a slab function is a line bundle on the toric variety defined by the normal fan of τ. The line bundle defined on τ is determined by the monodromy around the singular locus in the affine structure on B, see [20] for full details.

The Gross–Siebert algorithm iteratively refines the polyhedral decomposition $\mathscr{P}$ to $\mathscr{P}_k$, adding polyhedral objects called *walls*[7] $\mathfrak{d}$ which are equipped with functions $f_\mathfrak{d}$. The algorithm creates new walls for each $k \in \mathbb{Z}_{\geq 0}$ and for a given k the collection of walls and slabs is called a *structure* $\mathscr{S}_k$. The process of subdivision at each order defined in [20] ensures that the structure is, in the terminology of [20], *compatible*. Given a compatible structure Gross–Siebert define a functor F_k from a category defined using of $\mathscr{P}_k$, called $\underline{\mathrm{Glue}}(\mathscr{S}, k)$, to the category of rings. Objects of $\underline{\mathrm{Glue}}(\mathscr{S}, k)$ are certain triples $(\omega, \tau, \mathfrak{u})$ where ω and τ are strata of $\mathscr{P}$ and $\mathfrak{u} \in \mathrm{Chambers}(\mathscr{S}, k)$, the maximal cells of $\mathscr{P}_k$. The ring $F_k(\omega, \tau, \mathfrak{u})$ is denoted $R^k_{\omega,\tau,\mathfrak{u}}$, see [15, 20] for a complete definition. It is proved in [20] that, taking the inverse limit over this system of rings, a compatible structure defines a flat formal deformation of the reducible union of toric varieties whose moment polytopes are the maximal cells of $\mathscr{P}$.

The main tool used in [20] to construct the walls of $\mathscr{S}_k$ is the notion of *scattering diagram*. The only examples of scattering diagrams we shall use are the most basic studied and are studied in detail in [18, 19], to which we refer for details.

Definition 4.2. Given $s \in \mathbb{Z}_{>0}$ we fix the scattering diagram,

$$\mathfrak{D}(s) = \{(\mathbb{R}(1,0), 1 + tx^s), (\mathbb{R}(0,1), 1 + ty^s)\}.$$

[7] In the two-dimensional case these are also called *rays*.

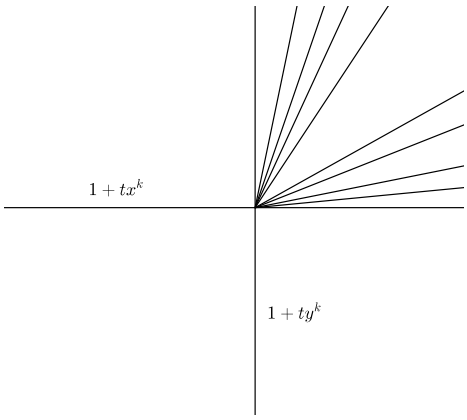

FIGURE 4.1. Rays of a scattering diagram $\mathfrak{D}_k(s)$.

Scattering diagrams 'localise' the problem of finding a compatible structure to achieving a certain consistency condition for each scattering diagram by adding new rays for each $k \in \mathbb{Z}_{\geq 0}$. The constructive proof that any scattering diagram can be made consistent by adding rays is due to Kontsevich–Soibelman [25]. The rays added to $\mathfrak{D}(s)$ by the scattering process admit a periodicity, resulting in a recursive formula identical to that found in Lemma 3.6. Let $\mathfrak{D}_k(s)$ denote the scattering diagram after adding rays to order k to $\mathfrak{D}(s)$; Figure 4 illustrates the supports of these rays. As we have seen, the gradients of these rays converge to values which are, in general, different. In the region between these asymptotes there are non-zero functions supported on rays of any rational slope.

There is an obvious parallel to be drawn with the collection of rays we considered from the mutating family of triangles in Section 3. In particular outside the region defined by the two asymptotes the recursive formulae for generating the support of the rays are identical.

Proposition 4.3. *Fix a triangle P and put it in standard form with respect to a vertex v. The collection of rays $\left\{\mathfrak{d}^i_j : i \in \{1,2\}, 1 \leq j\right\}$ formed in the construction described in Section 3 is equal to:*

$$\left\{(\mathfrak{d}, f_{\mathfrak{d}}) \in \mathfrak{D}(s) : g_{\mathfrak{d}} > \frac{s+\sqrt{s^2-4}}{2} \text{ or } g_{\mathfrak{d}} < \frac{s-\sqrt{s^2-4}}{2}\right\},$$

where s is the determinant of the map ρ and $g_{\mathfrak{d}}$ is the gradient of $\mathfrak{d}$.

Proof. Both collections of rays are generated by the same recursive formula, and have the same initial configuration. □

Remark 4.4. While the association of this set of rays with the triangles of the previous section seems mysterious, it is in fact tautological given the connection that both concepts have with cluster algebras. The relationship between combinatorial mutation and cluster algebras is explored in [23] and the deep connections between scattering diagrams and cluster algebras are explored in [18].

As well as the notion of a scattering diagram we will utilize the notion of a *broken line* from [8, 14]. These will provide an enumerative interpretation of the Laurent polynomials mirror to $\mathbb{P}^2$ as described in Theorem 1.3. The notion of broken line is very close to that of a *tropical disc*: broken lines can *bend* on the walls of a scattering diagram and one can

canonically complete these bends so that the resulting object is a tropical curve *with stops* (following the terminology of [28]). For more details see Lemma 5.4 of [8].

The idea of calculating a superpotential tropically, utilising broken lines in the affine manifold, was first explored in [8]. In Section 6 we show that there is a domain U in the dual intersection complex $B^\vee$ for a toric degeneration of $(\mathbb{P}^2, E)$ such that the tropically defined superpotential is equal to the family of Laurent polynomials described in [2].

In an ideal setting tropical curves should be the 'spines' of images of holomorphic curves under a special Lagrangian torus fibration. Tropical discs are similar, but now the curve has boundary so a 'stop' is introduced where the tropical disc terminates. For a more detailed discussion of this point see [8, 14, 28]. There are many technical results in [8] showing that the tropical superpotential behaves well which we do not include here, but rather present a summary of those definitions and results required for the proof of Theorem 1.1. The results are presented for an affine manifold B satisfying the conditions imposed by [8], all such conditions are satisfied by the affine manifold $B^\vee_{\mathbb{P}^2}$.

Definition 4.5. A *broken line* is a proper continuous map

$$\beta\colon (-\infty, 0] \to B$$

with 'bends' at a sequence of points $-\infty = t_0 < t_1 < \cdots < t_r = 0$ such that $\beta|_{(t_j, t_{j+1})}$ is an affine map with image disjoint from the rays of $\mathscr{S}$.

Additionally a broken line carries a sequence of monomials $a_j z^{m_j}$ such that $\beta'(t) = \bar{m}_j$ which are naturally transported as sections of $\beta^{-1}P_\phi$. At a point $\beta(t_i) \in \tau$ for τ a one cell in $\mathscr{P}_k$ the monomial $a_j z^{m_j}$ defines a unique element in $R^k_{\tau,\tau,\mathfrak{u}}$ where $\beta(t_i - \epsilon) \in \mathfrak{u}$ for sufficiently small $\epsilon > 0$. The wall-crossing formula $\theta_{\mathfrak{u},\mathfrak{u}'}$ defines a collection of monomials with order $\leq k$; these are the *results of transport* of $a_j z^{m_j}$.

For the broken line β we require that $\mathfrak{u}' \neq \mathfrak{u}$ and that the monomial attached to β is a result of transport. We also insist that $a_1 = 1$ and that there is an unbounded 1-cell of $\mathscr{P}$ parallel to $\bar{m}_1$ for which m_1 has order zero.

While this records the important aspects of the definition the reader is referred to [8] for a systematic treatment of broken lines.

Given a general[8] point $p \in B$, denote the set of broken lines β with $\beta(0) = p$ by $\mathfrak{B}(p)$. For a given structure $\mathscr{S}_k$ on B, the ring $R^k_{\omega,\tau,\mathfrak{u}}$ and a general $p \in \mathfrak{u}$ we can produce the *superpotential at order* k as an element of $R^k_{\omega,\tau,\mathfrak{u}}$, taking

$$W^k_{\omega,\tau,\mathfrak{u}}(p) = \sum_{\beta \in \mathfrak{B}(p)} a_\beta z^{m_\beta}$$

In [8] the authors obtain various results for $W^k_{\omega,\tau,\mathfrak{u}}(p)$, two of which we shall utilize in Section 6:

- The superpotential $W^k_{\omega,\tau,\mathfrak{u}}(p)$ is independent of the choice of $p \in \mathfrak{u}$ (Lemma 4.7 of [8]).
- The superpotentials are compatible with changing strata and chambers (Lemma 4.9 of [8]).

The content of the second point here is that, applying a change of chamber map to the superpotential, one obtains

$$\theta_{\mathfrak{u},\mathfrak{u}'}(W^k_{\omega,\tau,\mathfrak{u}}) = W^k_{\omega,\tau,\mathfrak{u}'}$$

where we have suppressed the dependence of $W^k_{\omega,\tau,\mathfrak{u}}(p)$ on p using the first point. This formula means that the superpotential changes by algebraic mutation discussed in Remark 2.4. To see this, we need to compare the rings $R^k_{\omega,\tau,\mathfrak{u}}$ and $\mathrm{k}[M]$ of which the respective superpotentials are elements. In Section 6 we shall find that the superpotential

[8]This is a generic condition, see Proposition 4.4 and Definition 4.6 of [8] for details.

$W^k_{\omega,\tau,\mathfrak{u}}$ is, in the terminology of [8], *manifestly algebraic* in a domain U we shall specify. The main conseqence of this is that the limit

$$W = \lim_{\leftarrow} W^k$$

is a *finite* sum. Recall that $R^k_{\omega,\tau,\mathfrak{u}}$ is a localisation of

$$\mathrm{k}[P_{\phi,\omega}]/I^k_{\omega,\tau,\sigma_{\mathfrak{u}}}$$

So for sufficiently large k the obvious lift of $W^k_{\omega,\tau,\mathfrak{u}}$ to $\mathrm{k}[P_{\phi,\omega}]$ is independent of k. In fact, to make this precise, we will also show that $\mathscr{P}_k$ can be chosen so that $\mathfrak{u}$ is not further subdivided as $k \to \infty$. Taking the projection $\mathrm{k}[P_{\phi,\omega}] \to \mathrm{k}[M]$ induced by setting $t = 1$, we can represent W as a single Laurent polynomial.

Lemma 4.6. *The wall crossing formulae*

$$\theta^k_{\mathfrak{u},\mathfrak{u}'}(z^m) = z^m \prod f_{\mathfrak{d}}^{\langle n, \bar{m}\rangle}$$

define birational maps $\theta^k_{\mathfrak{u},\mathfrak{u}'} \colon \mathrm{k}(M) \to \mathrm{k}(M)$. *If there is only a single ray supported on* $\mathfrak{d}$ *and* $f_{\mathfrak{d}} = 1 + c_m z^m$ *for some exponent* m *then the birational map* $\theta^k_{\mathfrak{u},\mathfrak{u}'}$ *is an* algebraic mutation *with factor polynomial* $(1 + c_m z^{\bar{m}})$.

Thus the result of *crossing a wall* is that the function recorded at the base point, viewed simply as a Laurent polynomial, undergoes a birational change of variables which is precisely the mutation with factor given by the line segment in the direction of the wall. This is an essential ingredient in the proof of Theorem 1.2 since it will allow us to compute the superpotential in every chamber from a calculation of broken lines in a single chamber.

5. The Affine Manifold $B^\vee_{\mathbb{P}^2}$

We now consider the affine structure on the dual intersection complex for a toric degeneration of $\mathbb{P}^2$. This is described in Example 2.4 of [8]. In [8], the authors consider the affine structure on the intersection complex and dual intersection complex of a so-called *distinguished* toric degeneration $(\mathfrak{X} \to T, \mathfrak{D})$. Given the pair $(\mathbb{P}^2, E)$ for a smooth genus one curve E, a distinguished toric degeneration will give an intersection complex as shown in Figure 1.1, as shown in the proof of Theorem 6.4 in [8].

For a precise definition of the discrete Legendre duality between $B_{\mathbb{P}^2}$ and $B^\vee_{\mathbb{P}^2}$ see [20]. Rather than provide this definition here we will describe $B^\vee_{\mathbb{P}^2}$ as an affine manifold. The manifold $B^\vee_{\mathbb{P}^2}$ was described in [8] and is shown in Figure 5.1. The affine manifold $B_{\mathbb{P}^2}$ associated to the *intersection* complex is shown in Figure 1.1. The affine structure on $B^\vee_{\mathbb{P}^2}$ is such that the three 'outgoing' unbounded 1-cells of $\mathscr{P}$ are parallel to each other, the dual condition to the requirement that $B_{\mathbb{P}^2}$ have smooth (flat) boundary. Charts may be formed as usual, by cutting along the invariant lines of each focus-focus singularity. Note that each such charts will in general be disconnected, so we replace each such chart with its connected component containing the unique closed 2-cell of $\mathscr{P}$.

Remark 5.1. Following the work of Gross–Hacking–Keel for log Calabi–Yau manifolds [16, 17] one might attempt to consider the affine manifold obtained by regarding all the singularities of $B^\vee_{\mathbb{P}^2}$ as lying at the origin, which would be the 'U^{trop}' in those papers, for a log Calabi–Yau U. However in this case we do not have *maximal boundary*: the resulting affine manifold is a single ray and does not fit easily into this framework.

Following the Gross–Siebert program [20], we endow the 1-cells τ of B supporting Δ with functions f_τ, or more precisely sections of $\mathcal{P}_\phi$ restricted to τ, defining a *log-structure* on a union of toric varieties. We shall make the standard choices of normalisation here so

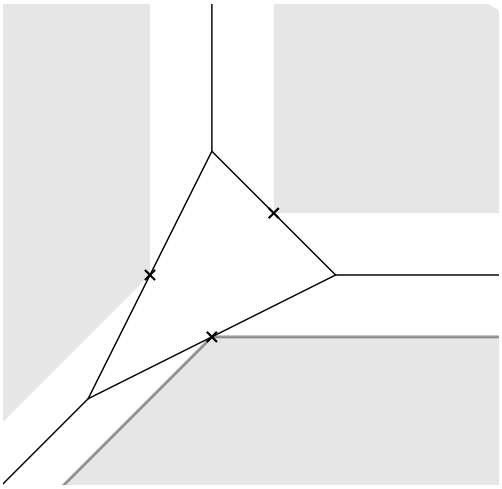

FIGURE 5.1. Affine structure on the dual intersection complex $B^\vee_{\mathbb{P}^2}$

that f_τ is $(1 + z^m)$ where m is an exponent[9] such that $\bar{m}$, a section of $\Lambda|_\tau$, is primitive and lies in the direction in τ *toward* the focus-focus singularity.

The data of $(B, \mathscr{P})$ together with the log-structure defines an initial structure, $\mathscr{S}_0$. Following the Gross–Siebert algorithm we shall consider various scattering diagrams in order to construct $\mathscr{S}_k$ for each k. In fact in Section 6 we shall compute a collection of regions using mutation of polygons and argue by our comparison result, Proposition 4.3, that this is the support of the union of scattering diagrams, away from a region densely filled with rays.

To compute the superpotential, we will use Corollary 6.8 of [8], which states that, for a base point in the interior of the bounded cell of $\mathscr{P}$, the superpotential for this structure is given by the usual Givental/Hori–Vafa superpotential:

$$W = x + y + \frac{1}{xy}$$

Each term here coming from a different broken line as shown in Figure 5.2. Using Lemma 4.9 of [8] this calculation determines the superpotential in every other chamber, using the wall-crossing formula $\theta_{\mathrm{u},\mathrm{u}'}$ to change chambers.

6. The Proof of Theorem 1.1

To prove Theorem 1.1 we will inductively build regions $U_n \supset U_{n-1}$ covered by the triangles corresponding to vertices of $\mathcal{G}$ with distance $\leq n$ from $(1, 1, 1)$, by considering new complexes $\mathrm{Diag}(P, v, k)$ at each stage. Defining $U := \lim_{n\geq 0} U_n$, we show that U is covered by (infinitely many) triangular regions and that the set of rays determined by the edges of these triangles is identical to the set of support of rays $\mathfrak{d}$ of the structure $\mathscr{S}$ intersected with U.

We shall define the domains U_k together with a polyhedral decomposition by induction. Indeed, define $U_0 = \mathrm{int}\,(P)$ the bounded 2-cell in $B^\vee_{\mathbb{P}^2}$ and consider $\mathrm{Diag}(P, v, 1)$ for each vertex $v \in \mathrm{verts}\,(P)$. While the affine structure on $B^\vee_{\mathbb{P}^2}$ is not trivial we can compose $\iota_{P,v,k}$ with a chart on $B^\vee_{\mathbb{P}^2}$ which contains v. Thus we define U_1 as the interior of the union of

[9]We recall from [20] that an *exponent* is a section of an extension of the local system (on B_0) of integral tangent vectors Λ by the constant sheaf $\underline{\mathbb{Z}}$. For an exponent m, let denote $\bar{m}$ denote the image of m in Λ.

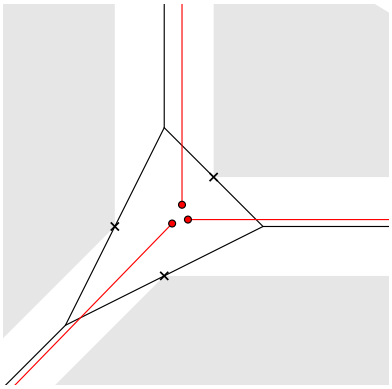

FIGURE 5.2. Broken lines in the central region

chambers $\mathfrak{u}^i_{1,1}$ for each vertex $v \in \mathrm{verts}\,(P)$ (this gluing is shown in Figure 1(a)). Observe that pairs of these chambers are identified by the transition functions on $B^\vee_{\mathbb{P}^2}$; there is only one additional chamber in U_1 for each edge of P. Also note that each $\mathfrak{u} = \mathfrak{u}^i_{1,1}$ has a distinguished vertex $v_\mathfrak{u}$ which is disjoint from $\bar{U}_0$.

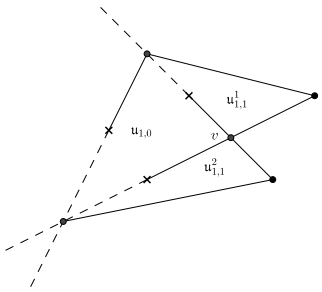

(a) Gluing in a diagram

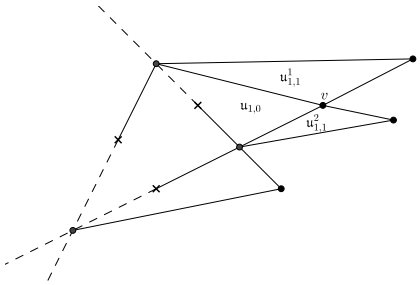

(b) Gluing a second $\mathrm{Diag}(P, v, 1)$

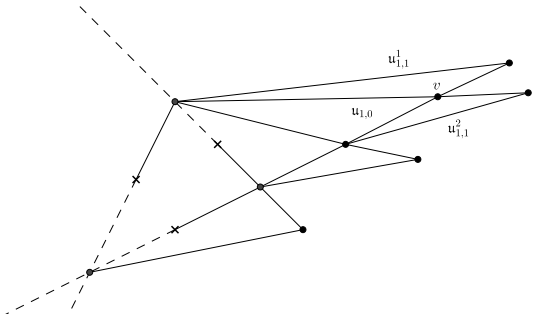

(c) Gluing a third $\mathrm{Diag}(P, v, 1)$

FIGURE 6.1. Building up $\mathrm{Chambers}(\mathscr{S}, k)$ using polygon mutation

Given $k > 0$ we consider the set

$$A_k = \{\mathfrak{u} \in \text{Chambers}(\bar{U}_k) \setminus \text{Chambers}(\bar{U}_{k-1})\}$$

where $\text{Chambers}(U_k)$ is the set of maximal cells of the underlying complex of $\bar{U}_k$. We form U_{k+1} as follows:

(1) By induction, there is a unique vertex $v_{\mathfrak{u}} \in \text{verts}(\mathfrak{u})$ for each $\mathfrak{u} \in A_k$ such that $v_{\mathfrak{u}}$ is not contained in $\bar{U}_k$.
(2) For every $\mathfrak{u} \in A_k$ form the diagram $\text{Diag}(\mathfrak{u}, v_{\mathfrak{u}}, 1)$.
(3) Embed $\text{Diag}(\mathfrak{u}, v_{\mathfrak{u}}, 1)$ into $B^{\vee}_{\mathbb{P}^2}$ by composing $\iota_{\mathfrak{u},v_{\mathfrak{u}},1}$ with a chart of $B^{\vee}_{\mathbb{P}^2}$; identifying $\mathfrak{u}$ with the corresponding chamber in $\bar{U}_k$.
(4) Identify those chambers with the same image in $B^{\vee}_{\mathbb{P}^2}$. Thus we form a complex $\bar{U}_{k+1}$ consisting of chambers each of which has a unique vertex $v_{\mathfrak{u}}$ disjoint from $\bar{U}_k$. Let U_{k+1} be the interior of the closed set $\bar{U}_{k+1}$.

Examples of this gluing process are shown in Figure 6.1. Observe that, using Construction 3.11, fixing a pair $(\mathfrak{u}, v_{\mathfrak{u}})$, as $k \to \infty$, this process generates all of $\text{Diag}(\mathfrak{u}, v_{\mathfrak{u}}, l)$ *for any* $l > 0$.

By the comparison result Proposition 4.3, every line segment appearing from this construction is a segment of a ray generated by a scattering diagram at a joint. This process also prolongs each of these segments of rays of the scattering diagram until they leave the domain U. The bound from Proposition 3.9 on their slope ensures they never enter U again. Combining these observations the proof is then reduced to a series of exercises.

(1) Each new edge produced by the chambers $\mathfrak{u}^i_{1,1}$ of $\text{Diag}(\mathfrak{u}, v_{\mathfrak{u}}, 1)$ is either an extension of an existing edge or a segment of a ray of the scattering diagram at one of the *other two* vertices of $\mathfrak{u}$.
(2) Every ray is prolonged until it enters the region between the two asymptotes in a unique diagram $\text{Diag}(\mathfrak{u}, v, k)$.
(3) An initial segment of every ray in the structure $\mathscr{S}$ intersected with U is produced for some k.

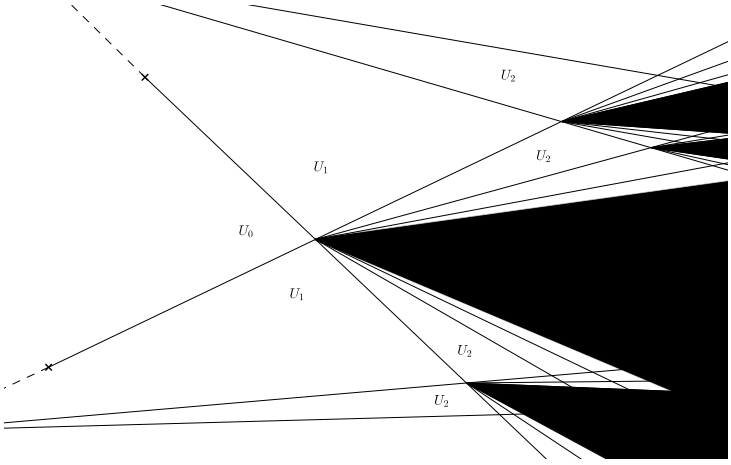

FIGURE 6.2. Part of U_2, defined by scattering diagrams in $\mathscr{S}$

For every $k \geq 0$ the chambers contained in U_k are stable (that is, they undergo no further subdivision as k increases) we combine this with the discussion of broken line counting in Section 4 to conclude that, since the superpotential is manifestly algebraic in the central chamber P of U and the functions attached to each rays are of the form

$1 + z^m$, the effect of the wall crossing formula is precisely an algebraic mutation. Since all Laurent polynomial mirrors to $\mathbb{P}^2$ are obtained by mutating from the polynomial $x+y+\frac{1}{xy}$ and by Theorem 1.1 we can exhibit any sequence of mutations of this polynomial by wall crossings have proved Theorem 1.2.

7. Acknowledgements

We thank Alexander Kasprzyk and Mohammad Akhtar for explaining combinatorial mutations and thank Tom Coates for suggesting a number of corrections. There is also a clear intellectual debt owed to the preliminary version of the paper [8] of Carl–Pumperla–Siebert. TP is supported by an EPSRC Postdoctoral Prize Fellowship.

References

[1] M. Akhtar, T. Coates, A. Corti, L. Heuberger, A. Kasprzyk, A. Oneto, A. Petracci, T. Prince, and K. Tveiten. Mirror symmetry and the classification of orbifold del pezzo surfaces. *preprint arXiv:1501.05334*, 2015.

[2] M. Akhtar and A. Kasprzyk. Mutations of fake weighted projective planes. *preprint math.AG/1302.1152*, 2013.

[3] M. Akhtar and A. Kasprzyk. Singularity content. *preprint: math.AG/1401.5458*, 2014.

[4] Mohammad Akhtar, Tom Coates, Sergey Galkin, and Alexander M. Kasprzyk. Minkowski polynomials and mutations. *SIGMA Symmetry Integrability Geom. Methods Appl.*, 8:Paper 094, 17, 2012.

[5] Denis Auroux. Mirror symmetry and T-duality in the complement of an anticanonical divisor. *J. Gökova Geom. Topol. GGT*, 1:51–91, 2007.

[6] Denis Auroux. Special Lagrangian fibrations, wall-crossing, and mirror symmetry. In *Surveys in differential geometry. Vol. XIII. Geometry, analysis, and algebraic geometry: forty years of the Journal of Differential Geometry*, volume 13 of *Surv. Differ. Geom.*, pages 1–47. Int. Press, Somerville, MA, 2009.

[7] Denis Auroux, Ludmil Katzarkov, and Dmitri Orlov. Mirror symmetry for weighted projective planes and their noncommutative deformations. *Ann. of Math. (2)*, 167(3):867–943, 2008.

[8] M. Carl, M. Pumperla, and B. Siebert. A tropical view on Landau Ginzburg models. *unpublished (preliminary version)*, 2011.

[9] Cheol-Hyun Cho and Yong-Geun Oh. Floer cohomology and disc instantons of Lagrangian torus fibers in Fano toric manifolds. *Asian J. Math.*, 10(4):773–814, 2006.

[10] Tom Coates, Alessio Corti, Sergey Galkin, Vasily Golyshev, and Alexander M. Kasprzyk. Mirror symmetry and Fano manifolds. In *European Congress of Mathematics Kraków, 2–7 July, 2012*, pages 285–300, 2014.

[11] Alexander Givental. Homological geometry and mirror symmetry. In *Proceedings of the International Congress of Mathematicians, Vol. 1, 2 (Zürich, 1994)*, pages 472–480. Birkhäuser, Basel, 1995.

[12] Alexander Givental. Stationary phase integrals, quantum Toda lattices, flag manifolds and the mirror conjecture. In *Topics in singularity theory*, volume 180 of *Amer. Math. Soc. Transl. Ser. 2*, pages 103–115. Amer. Math. Soc., Providence, RI, 1997.

[13] Alexander Givental. A mirror theorem for toric complete intersections. In *Topological field theory, primitive forms and related topics (Kyoto, 1996)*, volume 160 of *Progr. Math.*, pages 141–175. Birkhäuser Boston, Boston, MA, 1998.

[14] Mark Gross. Mirror symmetry for $\mathbb{P}^2$ and tropical geometry. *Adv. Math.*, 224(1):169–245, 2010.

[15] Mark Gross. *Tropical geometry and mirror symmetry*, volume 114 of *CBMS Regional Conference Series in Mathematics*. Published for the Conference Board of the Mathematical Sciences, Washington, DC; by the American Mathematical Society, Providence, RI, 2011.

[16] Mark Gross, Paul Hacking, and Sean Keel. Birational geometry of cluster algebras. *Algebr. Geom.*, 2(2):137–175, 2015.

[17] Mark Gross, Paul Hacking, and Sean Keel. Mirror Symmetry for log Calabi-Yau surfaces I. *Publications mathematiques de l'IHES*, 2015.

[18] Mark Gross, Paul Hacking, Sean Keel, and Maxim Kontsevich. Canonical bases for cluster algebras. `arXiv:1411.1394 [math.AG]`, 2014.

[19] Mark Gross, Rahul Pandharipande, and Bernd Siebert. The tropical vertex. *Duke Math. J.*, 153(2):297–362, 2010.

[20] Mark Gross and Bernd Siebert. From real affine geometry to complex geometry. *Ann. of Math. (2)*, 174(3):1301–1428, 2011.

[21] Paul Hacking and Yuri Prokhorov. Smoothable del Pezzo surfaces with quotient singularities. *Compos. Math.*, 146(1):169–192, 2010.
[22] K. Hori and C. Vafa. Mirror symmetry. `arXiv:hep-th/0002222`, 2000.
[23] A. Kasprzyk, B. Nill, and T. Prince. Minimality and mutation-equivalence of polygons. `arXiv:1501.05335 [math.AG]`, 2015.
[24] Ludmil Katzarkov and Victor Przyjalkowski. Landau-Ginzburg models—old and new. In *Proceedings of the Gökova Geometry-Topology Conference 2011*, pages 97–124. Int. Press, Somerville, MA, 2012.
[25] Maxim Kontsevich and Yan Soibelman. Affine structures and non-Archimedean analytic spaces. In *The unity of mathematics*, volume 244 of *Progr. Math.*, pages 321–385. Birkhäuser Boston, Boston, MA, 2006.
[26] Grigory Mikhalkin. Counting curves via lattice paths in polygons. *C. R. Math. Acad. Sci. Paris*, 336(8):629–634, 2003.
[27] Grigory Mikhalkin. Enumerative tropical algebraic geometry in $\mathbb{R}^2$. *J. Amer. Math. Soc.*, 18(2):313–377, 2005.
[28] Takeo Nishinou. Disk counting on toric varieties via tropical curves. *Amer. J. Math.*, 134(6):1423–1472, 2012.
[29] Takeo Nishinou and Bernd Siebert. Toric degenerations of toric varieties and tropical curves. *Duke Math. J.*, 135(1):1–51, 2006.
[30] T. Prince. Smoothing toric Fano surfaces using the Gross–Siebert algorithm. `arXiv:1504.05969 [math.AG]`, 2015.
[31] Helge Ruddat. Mirror duality of Landau-Ginzburg models via discrete Legendre transforms. In *Homological mirror symmetry and tropical geometry*, volume 15 of *Lect. Notes Unione Mat. Ital.*, pages 377–406. Springer, Cham, 2014.
[32] Paul Seidel. More about vanishing cycles and mutation. In *Symplectic geometry and mirror symmetry (Seoul, 2000)*, pages 429–465. World Sci. Publ., River Edge, NJ, 2001.
[33] Paul Seidel. Vanishing cycles and mutation. In *European Congress of Mathematics, Vol. II (Barcelona, 2000)*, volume 202 of *Progr. Math.*, pages 65–85. Birkhäuser, Basel, 2001.
[34] Andrew Strominger, Shing-Tung Yau, and Eric Zaslow. Mirror symmetry is T-duality. *Nuclear Phys. B*, 479(1-2):243–259, 1996.
[35] Renato Vianna. On exotic Lagrangian tori in $\mathbb{CP}^2$. *Geom. Topol.*, 18(4):2419–2476, 2014.

Department of Mathematics, Imperial College London, London, SW7 2AZ, UK
E-mail address: `t.prince12@imperial.ac.uk`